JACS
JOURNAL OF THE AMERICAN CHEMICAL SOCIETY

Article

pubs.acs.org/JACS

Electronic Structure and Slow Magnetic Relaxation of Low-Coordinate Cyclic Alkyl(amino) Carbene Stabilized Iron(I) Complexes

Prinson P. Samuel,[†] Kartik Chandra Mondal,[†] Nurul Amin Sk,[†] Herbert W. Roesky,*[,†] Elena Carl,[†] Roman Neufeld,[†] Dietmar Stalke,*[,†] Serhiy Demeshko,[†] Franc Meyer,*[,†] Liviu Ungur,*[,‡] Liviu F. Chibotaru,[‡] Jonathan Christian,[§] Vasanth Ramachandran,[§] Johan van Tol,[∥] and Naresh S. Dalal*[,§,∥]

[†]Institut für Anorganische Chemie, Georg-August-Universität, Tammannstrasse 4, D-37077, Göttingen, Germany

[‡]KU Leuven, Celestijnenlaan, 200F, 3001, Leuven, Belgium

[§]Departments of Chemistry and Biochemistry and [∥]National High Magnetic Field Laboratory, Florida State University, 600 W College Ave, Tallahassee, Florida 32306, United States

Supporting Information

ABSTRACT: Cyclic alkyl(amino) carbene stabilized two- and three-coordinate Fe(I) complexes, $(cAAC)_2FeCl$ (**2**) and $[(cAAC)_2Fe][B(C_6F_5)_4]$ (**3**), respectively, were prepared and thoroughly studied by a bouquet of analytical techniques as well as theoretical calculations. Magnetic susceptibility and Mössbauer spectroscopy reveal the +1 oxidation state and $S = 3/2$ spin ground state of iron in both compounds. **2** and **3** show slow magnetic relaxation typical for single molecule magnets under an applied direct current magnetic field. The high-frequency EPR measurements confirm the $S = 3/2$ ground state with a large, positive zero-field splitting (~20.4 cm^{-1}) and reveal easy plane anisotropy for compound **2**. CASSCF/CASPT2/RASSI-SO *ab initio* calculations using the MOLCAS program package support the experimental results.

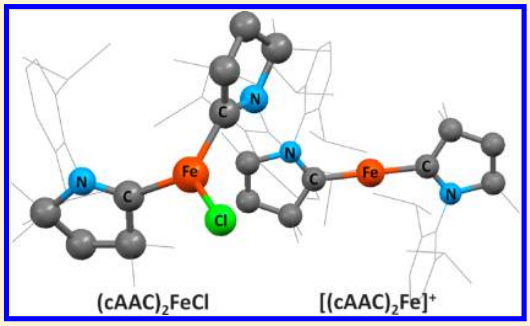

The chemistry of iron is of fundamental importance not only because of its highest abundance among the transition elements in the biosphere but also due to its variety of applications in chemical industry. In nature, iron containing enzymes are involved in catalyzing many redox reactions where the electron transfer is facilitated by switching the oxidation state of the iron center.[1] Oxidation states of known iron complexes vary from −2 to +6, but the most common among them are the ferric (Fe^{3+}) and ferrous (Fe^{2+}) compounds. In terms of coordination geometry, octahedral complexes constitute the largest class of iron compounds even though complexes with lower-coordinate iron are also well-known. However, only a limited number of complexes with three- and two-coordinate iron centers have been prepared.[2] The interest in such complexes with low-coordinate iron atoms stems from their potential to exhibit unusual reactivities and magnetic properties. It should be noted that the iron centers present in the isolated protein pockets of metalloenzymes (e.g., ribonucleotide reductase and nitrogenase) have only a limited number of potential donors.[3] Nature's intelligent choice of placing low-coordinate metal atoms in such isolated pockets have been mimicked by chemists by employing bulky ligands whose steric restrictions prevent metal atoms from achieving high-coordination polyhedra.[2,4]

Bradley reported the X-ray structure of $Fe[N(SiMe_3)_2]_3$, the first complex with a three-coordinate Fe(III) ion.[5] Later on, rigorously bulky ligands were employed by Power and Shoner[6] and others[7] for synthesizing a number of complexes with three-coordinate Fe(II) ions. In the past decade, the chemistry of complexes with three-coordinate iron(II) was extensively studied by Holland et al. using β-diketiminate ligands.[2a,8] In contrast, the chemistry of compounds with low-coordinate Fe(I) is still in its infancy, and understanding the properties of such compounds is of fundamental interest. The earliest attempts to obtain low coordinate Fe(I) were the preparations of $[PhB(CH_2PPh_2)_3]Fe(PPh_3)$ and $[PhTp^{But}]Fe(CO)$ ($PhTp^{But}$ is a tris(pyrazolyl)borato ligand), the complexes with four-coordinate Fe(I).[9] Subsequently, complexes with three-coordinate Fe(I) were reported by Holland et al. using β-diketiminate ligands.[10] Interestingly, complexes of three-coordinate Fe(I) ($[\{KLFeH\}_2]$ and $[KLFe]_2(\mu\text{-}S)$, L = β-diketiminate) were obtained by the one-electron reduction of Fe(II) ions in the respective precursor compounds ($[\{LFe(\mu\text{-}H)\}_2]$ and $[\{LFe\}_2(\mu\text{-}S)]$) using potassium.[11] All these compounds share the common features that the Fe(I) ion is well buried in the steric protection of bulky ligands and the

Received: April 30, 2014
Published: July 29, 2014

   dx.doi.org/10.1021/ja5043116 | J. Am. Chem. Soc. 2014, 136, 11964−11971

ligands are anionic and chelating. These features restrict the Fe(I) complexes from further functionalization, whereas the reactivity studies would be greatly facilitated in the case of easily substitutable groups like halides at the Fe(I) center. At the same time, only one complex with a two-coordinate iron(I) is known so far; that is the anionic complex $[Fe(C(SiMe_3)_3)_2]^-$ reported by Long and coworkers.[12a] This linear complex was found to exhibit slow magnetic relaxation below 29 K in a zero applied direct-current (dc) field. An effective spin-reversal barrier of 226(4) cm^{-1} and magnetic blocking below 4.5 K were observed for this compound. Such single molecule magnets (SMM) attract attention because they are uniquely advantageous to serve as new tools to test magnetic theories and to understand new magnetic phenomena in the quantum regime.[12b]

This scenario of Fe(I) compounds raised our interest in utilizing cyclic alkyl(amino) carbenes (cAACs) for the synthesis of complexes with three- and two-coordinate Fe(I) centers, though a cAAC stabilized complex with four-coordinate Fe(II) was recently reported.[13a] cAACs are not only less bulky compared to the conventional ligands used in low-coordinate iron chemistry but also have been proven to stabilize transition metals in low oxidation states.[13b] Here we report that reducing $(cAAC)_2Fe(II)Cl_2$ (**1**) with 1 equiv of KC_8 leads to the formation of $(cAAC)_2Fe(I)Cl$ (**2**), the first complex in which Fe(I) is stabilized in a three-coordinate nonchelating ligand environment. The reaction of **2** with $Li[B(C_6F_5)_4]\cdot 2.5Et_2O$ yields $[(cAAC)_2Fe]^+[B(C_6F_5)_4]^-$ (**3**), the first cationic complex with a two-coordinate Fe(I) center.

Scheme 1. Syntheses of Compounds 1−3

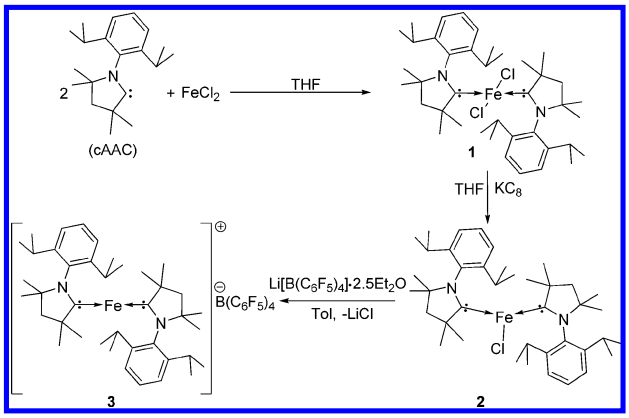

Tetrahedral compound **1** was synthesized by reacting $FeCl_2$ with 2 equiv of cAAC in THF (see SI for details of the molecular structure of **1**). The reaction of **1** with 1 equiv of KC_8 in THF resulted in the formation of **2** in good yield. A saturated solution of **2** at −18 °C afforded crystals suitable for X-ray diffraction.[14] **2** crystallizes in the monoclinic space group $P2_1/c$. The geometry around the Fe atom is trigonal planar with an angular sum at Fe of 359.96 ° (Figure 1). The average Fe−C distance is 1.9968 Å which is shorter than the corresponding bond length in **1** (2.1496 Å). However, there was no significant shortening of the Fe−Cl bond in **2** (2.2519(4)) when compared to the average Fe−Cl bond length in **1** (2.2809 Å). **2** is stable only in inert atmosphere, and it decomposes on exposure to air in a few minutes. It is interesting to note that the Fe−Cl part is not surrounded by bulky groups, and this

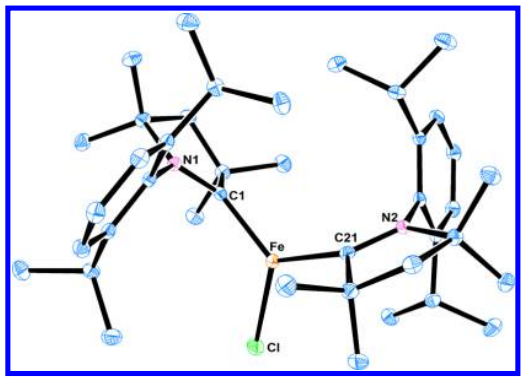

Figure 1. Molecular structure of **2**. Hydrogen atoms are omitted for clarity. Anisotropic displacement parameters are depicted at the 50% probability level. Selected bond lengths [Å] and angles [°] Fe−C1, 1.9816(13); Fe−C21, 2.0121(13); Fe−Cl, 2.2519(4); C1−N1, 1.3430(16); C21−N2, 1.3324(16); C1−Fe−Cl, 119.62(4), C21−Fe−Cl, 119.45(4), C1−Fe−C21, 120.89(5).

leaves enormous scope for further reactivity studies of this compound.

2 reacts with $Li[B(C_6F_5)_4]\cdot 2.5Et_2O$ in toluene to afford **3** in very high yield. **3** is insoluble in toluene, has a shining blue color and is stable for several weeks in inert atmosphere. On exposure to air, it readily decomposes in the solid state as well as in solution. In an inert atmosphere **3** retains its blue color up to 145 °C, but turns irreversibly to gray on further heating. The crystals suitable for X-ray diffraction were obtained from a solution in fluorobenzene at −35 °C. **3** crystallizes in the triclinic space group $P\bar{1}$. The molecular structure shows that the Fe atom is ligated linearly (Figure 2; see also SI, Figure S2).

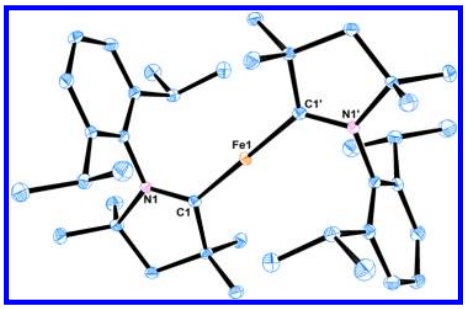

Figure 2. Structure of the cationic part of **3**. Hydrogen atoms are omitted for clarity. Anisotropic displacement parameters are depicted at the 50% probability level. Selected bond lengths [Å] and angles [°] Fe1−C1/Fe2−C1A, 1.999(2)/ 2.008(2); C1−N1/C1A−N1A, 1.315(2)/1.313(2); C1−Fe1−C1′, 180.

The Fe atom is located at the inversion center of $[(cAAC)_2Fe]^+$, the cation of **3**. The two symmetrically independent Fe−C bond distances of the two molecules in the asymmetric unit are 1.999(2) and 2.008(2) Å which is similar to the corresponding bond distances of **2**. (see SI, Figure S3)

A previously reported compound with four-coordinate iron ($[FeCl(iPrPDI)]$, iPrPDI = 2,6-(2,6-$iPr_2C_6H_3N{=}CMe)_2C_5H_3N$ is a tridentate neutral ligand) was presumed to contain a Fe(I) center but was later proven to be a Fe(II) compound with ground state spin $S = 3/2$ originating from the antiferromagnetic coupling of the Fe(II) center ($S = 2$) and a ligand centered radical ($S = 1/2$).[15] A similar spin−spin

dx.doi.org/10.1021/ja5043116 | J. Am. Chem. Soc. 2014, 136, 11964−11971

coupling was reported very recently for $(cAAC)_2Mn$ in which the ground state spin $S = 3/2$ results from antiferromagnetic coupling between the Mn(I) (d^6, $S = 2$) and one radical delocalized over the cAAC ligands ($S = 1/2$).[13] So it is crucial to investigate the exact electronic structures of **2** and **3** experimentally and theoretically. The Mössbauer spectrum of **2** is shown in Figure 3. The spectrum measured at 80 K shows a

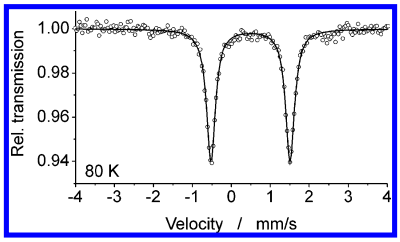

Figure 3. Mössbauer spectrum of **2** at 80 K.

quadrupole doublet characterized by an isomer shift of $\delta = 0.49$ mm s^{-1} and a quadrupole splitting of $\Delta E_Q = 2.02$ mm s^{-1} with the line width of $\Gamma = 0.27$ mm s^{-1}. At 6 K the isomer shift ($\delta = 0.51$ mm s^{-1}) and quadrupole splitting ($\Delta E_Q = 2.09$ mm s^{-1}) are almost equal to the corresponding values at 80 K, but the spectrum becomes significantly broader ($\Gamma = 0.54$ mm s^{-1}) indicating the incipient paramagnetic relaxation typical for half-integer spin systems[16] (see SI, Figure S4).

Mössbauer parameters and especially δ are highly sensitive to the oxidation state, coordination number, donor–acceptor properties of the ligand and can provide useful information about the electronic structure. Typical isomer shifts for complexes with three-coordinate Fe(II) lie in the range from 0.57 to 0.74 mm s^{-1}.[6d,8a,11b,17] Furthermore, the isomer shifts of low-coordinate Fe(I) complexes are usually more negative due to stronger π-back bonding than those of Fe(II) complexes.[12a,15] The δ value of 0.49 mm s^{-1} in **2** is very close to those of the diketiminate complexes $[\{KLFeH\}_2]$ and LFe(HCCPh) (0.40–0.48 mm s^{-1}) with three-coordinate Fe(I) but lower than that in $[\{KLFe\}_2(\mu\text{-S})]$ (0.64 to 0.67 mm s^{-1}).[10,11] Further indications of the Fe(I) state with $S = 3/2$ in **2** were obtained from magnetic susceptibility measurements (Figure 4).

The observed $\chi_M T$ value at rt is 2.93 cm^3 mol^{-1} K which is, as expected, much higher than the spin only value for $S = 3/2$ (1.875 cm^3 mol^{-1} K) due to significant orbital contribution as it was observed in other Fe(I) and isoelectronic Co(II) complexes.[12a,18] The $\chi_M T$ product remains nearly constant down to 50 K (Figure 4) and then decreases to 1.82 cm^3 mol^{-1} K at 2 K indicating a very large zero-field splitting. The spin state of $S = 3/2$ further supports the initial assumption of a +1 oxidation state of the iron atom drawn from the Mössbauer spectrum. It should be noted that no temperature dependence of $\chi_M T$ was observed from 50 K to rt, which means that the alternative electronic structure of a "carbene" radical ($S = 1/2$) coupling with an Fe(II) center ($S = 2$) would require extremely strong antiferromagnetic coupling. Drawing a final conclusion about the Fe oxidation state in **2** thus required complementary theoretical calculations (see below). Magnetic data analysis for **2** using an appropriate spin Hamiltonian with zero-field splitting and Zeeman interaction gave rise to a good fit with values of $g = 2.54$ and $|D| = 19.8$ cm^{-1}. Simulation of data obtained from the variable-temperature–variable-field (VTVH) magnetization measurements (Figure 4, inset) leads to essentially the same values $g = 2.57$ and $D = +20.4$ cm^{-1}; a small rhombic ZFS parameter E was included and fixed to $E/D = 0.01$. Recently, interesting magnetic properties such as slow relaxation of magnetization were recognized for d^7 single ion systems, e.g., Co(II) upon application of a dc magnetic field even if $D > 0$.[19] The alternating current (ac) magnetic susceptibilities under a dc magnetic field $H_{dc} = 500$ Oe indeed indicated SMM behavior of **2** (Figure 5). In the case of zero dc field no out-of-phase ac susceptibility (m'') signal was observed.

In order to extract the relaxation parameters, the frequency-dependent data were analyzed using an Arrhenius law according to eq 1:

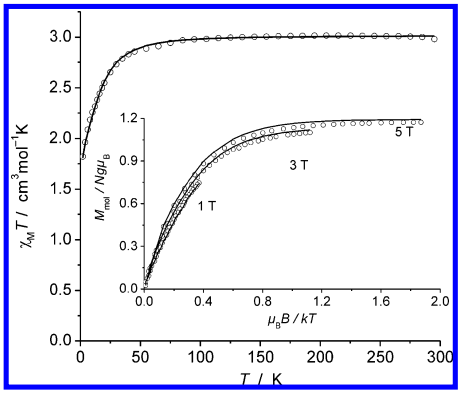

Figure 4. $\chi_M T$ versus T plot and VTVH magnetization measurements as M_{mol} versus B/T (inset) for **2**. Solid lines represent the calculated curve fits (see text).

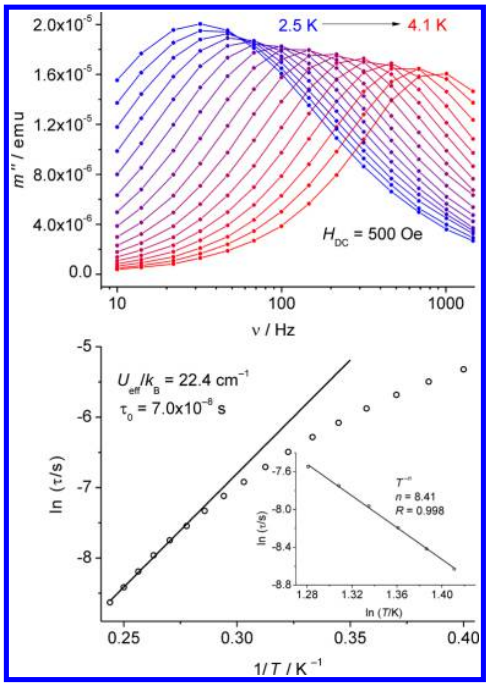

Figure 5. Top: Frequency dependence of the imaginary part of the ac susceptibility under a dc field of 500 Oe for **2**. Bottom: Arrhenius plot of the temperature dependence of the relaxation time τ. The black line describes a thermally activated relaxation. Inset: power law analysis in the form $\ln(\tau)$ vs $\ln(T)$.

dx.doi.org/10.1021/ja5043116 | J. Am. Chem. Soc. 2014, 136, 11964–11971

$$\tau = \tau_0 \exp(U_{eff}/k_B T) \quad (1)$$

A linear fit in the temperature range from 3.6 to 4.1 K led to the energy barrier U_{eff}/k_B = 22.4 cm^{-1} and the characteristic relaxation time $\tau_0 = 7.0 \times 10^{-8}$ s. The deviation from Arrhenius behavior at lower temperatures is most probably due to quantum tunnelling of the magnetization. The energy barrier is in the typical range (8.7−24 cm^{-1}) observed for complexes of isoelectronic Co(II) ion with S = 3/2 and positive D.[18,19,20] For the d^7 case with a large easy plane anisotropy (D > 0), the ground Kramers doublet M_s = ±1/2 is separated from the excited M_s = ±3/2 by an energy gap $U_{eff}/k_B = 2D$. Possible reasons for the occurrence of slow relaxation for such systems are (i) a field-induced bottleneck effect;[19] (ii) the presence of a large rhombic anisotropy barrier determined by the E parameter;[20b] or (iii) a dominant role of an optical acoustic Raman process.[20c] For possibility (i) the relaxation between M_s = ±1/2 via an Orbach pathway through the exited M_s = ±3/2 states should lead to an energy barrier of 2D or ∼40 cm^{-1}. The value obtained experimentally from ac susceptibility measurements (22.4 cm^{-1}) is much lower and does not support this explanation. The second possibility can be ruled out since the rhombic anisotropy E obtained from EPR experiments (see below) is very small. To further corroborate that explanation (iii) is valid in this case, the relaxation time was fitted to a T^{-n} law (Figure 5 (bottom), inset). The obtained value n = 8.41 is very close to the expected n = 9 for Raman relaxation in Kramers ions,[20c,d] strongly suggesting the dominant contribution of a Raman process for the spin relaxation in **2**.

Mössbauer spectra of **3** are provided in Figure 6. The spectrum measured at 80 K shows a quadrupole doublet

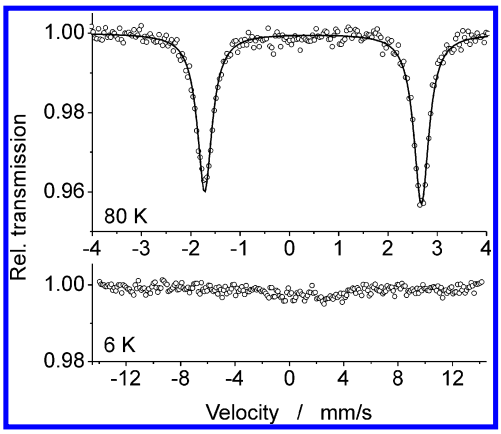

Figure 6. Mössbauer spectra of **3** at 80 K (top) and 6 K (bottom). See also Figure S5 in SI.

characterized by an isomer shift of 0.48 mm s^{-1} which is almost equal to the corresponding value for **2** and comparable to the data for a few previously reported two-coordinate Fe(I) and Fe(II) complexes (0.4 to 0.5 mm s^{-1} at $T \leq$ 80 K).[12a,21] Interestingly, the quadrupole splitting (ΔE_Q = 4.40 mm s^{-1}) is much larger than those for known linear Fe(II) (0.74−1.3 mm s^{-1})[21] or Fe(I) (2.56 mm s^{-1} at 5 K)[12a] complexes. The slight asymmetry of the doublet (intensity (left/right) = 0.93) can be attributed to a texture effect.[16] A spectrum recorded at 6 K indicates line broadening and probably magnetic splitting in six lines due to nuclear Zeeman effect beyond detection, likely because of slow paramagnetic relaxation at such low temperatures.

The S = 3/2 spin ground state of **3** is further evidenced by magnetic susceptibility measurements (Figure 7). The $\chi_M T$

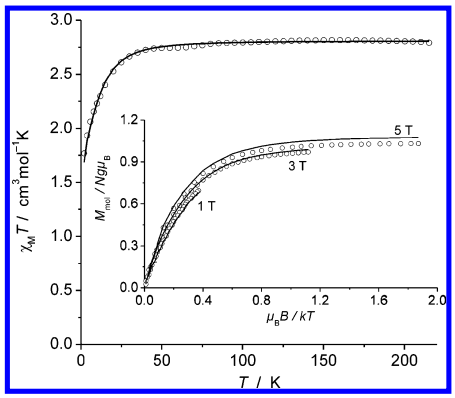

Figure 7. $\chi_M T$ versus T plot and VTVH magnetization measurements as M_{mol} versus B/T (inset) for **3**. Solid lines represent the calculated curve fits (see text).

value at rt is 2.79 cm^3 mol^{-1} K which is higher than the spin only value for S = 3/2 (1.875 cm^3 mol^{-1} K) but lower than for S = 2 (3.0 cm^3 mol^{-1} K). In all known linear Fe(II) complexes the observed $\chi_M T$ values are usually much higher than 3.0 cm^3 mol^{-1} K (up to 5.8 cm^3 mol^{-1} K),[21,22] so a spin state of S = 2 is not in accordance with the experimental data for **3**. No significant temperature dependence of $\chi_M T$ was observed from 50 to 215 K. Analysis of the $\chi_M T$ vs T curve for **3** leads to g = 2.45 and D = −13.6 cm^{-1}. Simulation of the data obtained from VTVH magnetization measurements (Figure 7, inset) gives a similar g = 2.50 and confirms the negative sign of D though the absolute value of D = −22.0 cm^{-1} is larger. Similar to **2**, a frequency-dependent maximum of the ac susceptibility typical for SMM behavior is found for **3** under an applied static magnetic field (Figure 8). The maxima are shifted to lower

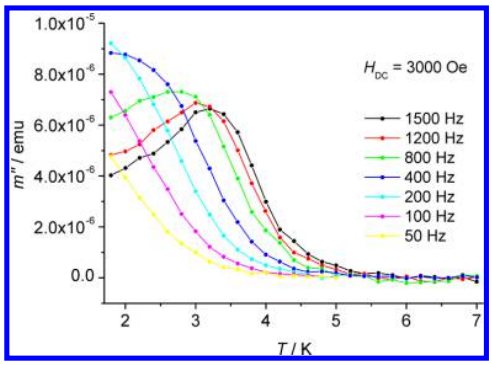

Figure 8. Frequency dependence of the imaginary part of the ac susceptibility of **3** under a dc field of 3000 Oe.

temperatures compared to **2** indicating a lower energy barrier. Since only a few data points at higher frequencies are available, from the Arrhenius law analysis we can only give an approximate value or upper limit for the energy barrier for **3**, U_{eff}/k_B < 20 cm^{-1}. This is more than 10 times lower than the barrier of the only previously reported linear Fe(I) complex [Fe(C(SiMe$_3$)$_3$)$_2$]$^-$ (226 cm^{-1}).[12a] The reason for this lies in the fundamentally different electronic structure of **3** compared to [Fe(C(SiMe$_3$)$_3$)$_2$]$^-$ (see below).

dx.doi.org/10.1021/ja5043116 | J. Am. Chem. Soc. 2014, 136, 11964−11971

The above results from SQUID data suggest that both **2** and **3** have large D values, *but with opposite signs.* This called for further measurements by an independent technique: the high-frequency electron paramagnetic resonance (HF-EPR) spectroscopy. We began measurements with **3**, since this two-coordinate Fe complex is a rather rare case, both in terms of geometry and the magnetic parameters deduced from the SQUID data (i.e., a very large and negative D). Computer simulations of the energy levels using a microwave frequency of 336 GHz (the highest frequency that was experimentally available to us) and $D = -13.6$ cm^{-1}, $S = 3/2$, and $g = 2.45$ are shown in Figure 9 (see SI for the spin Hamiltonian equation). The red arrows indicate the field values where the microwave quantum would fit resonantly $h\nu \sim g\beta H + D(2M_s + 1)$. In Fe complexes it is often necessary to cool the sample down to liquid helium temperatures in order to observe an EPR signal, because of the expected fast spin−lattice relaxation process,[20d] which can occur even in samples which exhibit slow magnetic relaxation.[23,24] This is because the time scales of EPR relaxation and magnetization relaxation are usually quite different in multilevel systems. Magnetization relaxation involves the crossing of the electron−spin over the entire (spin inversion) barrier. The underlying mechanism is usually either direct quantum tunneling of the magnetization vector or phonon-assisted tunneling, which are inherently slow processes. EPR relaxation, on the other hand, is within a given multiplet; and can be fast if the system has available a phonon bath, which is provided by the lattice. This is often the case with SMMs such as Mn_{12}-acetate, for which EPR signals are not detectable above about 30 K, but slow magnetization relaxation is observed below 4 K.[23,24]

Figure S6 shows that in low-temperature conditions the populated energy level of **3** would be the lowest one, but the transition between the two lowest levels would be strongly forbidden because it will involve $\Delta M_s = 3$. Moreover, in the case of H in the xy plane, the resonant levels 1 and 2 are so high that they would not be expected to be populated.

Thus, if the susceptibility analysis were correct, then little or no EPR should be expected for **3** using the available microwave frequencies of up to 336 GHz. Indeed, repeated efforts using variable-temperature (3−295 K) and variable-frequency (240 and 336 GHz) and modifying experimental parameters for optimum signal intensity (using EPR standards and complex **2**, *vide infra*) yielded no detectable EPR signals. This result points to two possibilities: either **3** is diamagnetic or the D value is negative and larger than 336 GHz.[11a,25] It is clear from the SQUID and Mössbauer data (vide supra) that this compound is definitely not diamagnetic; therefore, the latter explanation is the correct one; a result that strongly favors the correctness of the above-noted magnetic parameters for **3**. This conclusion was strengthened by our X-band measurements, at the low frequency of 9.4 GHz and magnetic fields below 0.8 T, and using an order of magnitude larger sample along with a Bruker high-Q resonant cavity. The observed spectra are presented in Figure S7. The spectra show three main peaks at 0.08 T, 0.22 and 0.38 T. Simulation of the spectra were quite consistent with the S, D, and g parameters deduced from the SQUID measurements.

HF-EPR measurements on **2** were performed under very similar experimental conditions as on **3**. Figure 9 shows experimentally observed and computer simulated EPR spectra for **2** at 336 GHz. Also shown are the simulated energy level diagrams for H along the principal symmetry axis of the molecule ($H \parallel z$) and along the perpendicular x, y directions (top and bottom segment respectively). EPR spectra were not observable above 20 K, likely due to fast spin−lattice relaxation.[26] Below 20 K three distinct g-tensor components are seen at $g_x' = 6.64$, $g_y' = 6.36$, and $g_z' = 2.91$. Such large anisotropy is the evidence of significant zero-field splitting, thus the g values are labeled with prime symbols indicating they are effective values. For $S = 3/2$ with a large D (i.e., $D \gg$ microwave quantum), the effective and real g values are related

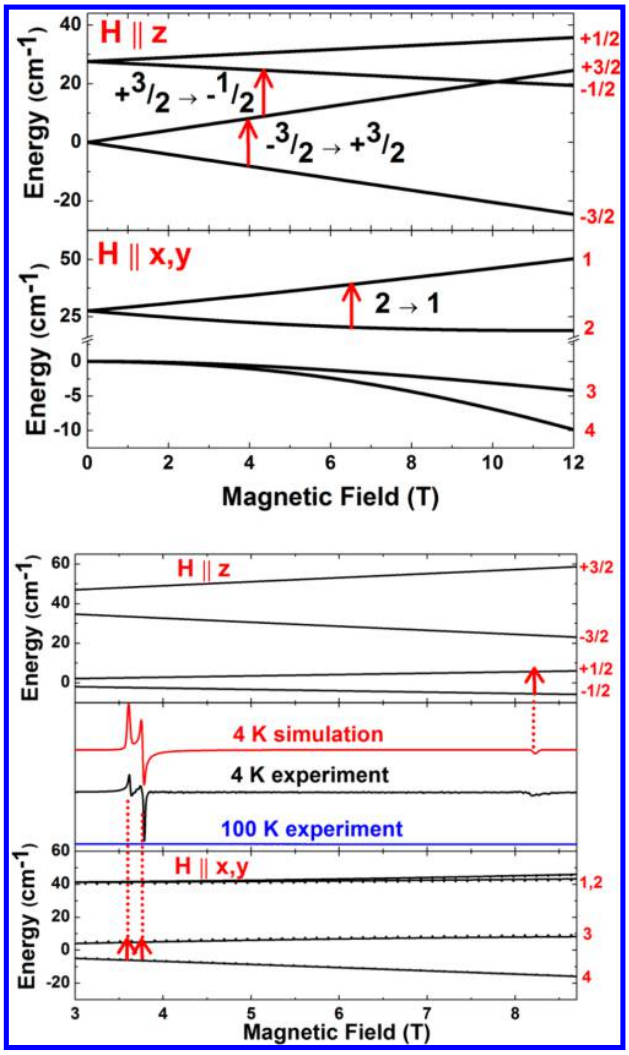

Figure 9. (Top): Calculated energy level diagrams for the $H \parallel z$ (principal symmetry axis of the molecule) and the perpendicular x, y directions using the parameters: $S = 3/2$, $D = -13.6$ cm^{-1}, and isotropic $g = 2.45$ for compound **3**. The red numbers in the top figure represent the M_s quantum numbers in the high-field limit. In the bottom figure however, they are just a label for an energy level since the field strength was not enough to be in the "high-field" limit. Red arrows indicate possible EPR transitions where the microwave quantum could fit resonantly, but the selection rule $\Delta M_s = \pm 1$ causes these transitions to be strongly forbidden in the standard EPR configuration ($H_\mu \perp H_{applied}$). (Bottom): Variable-temperature 336 GHz EPR experimental spectra and simulation for compound **2**. The top and bottom portions show the energy level diagram for the Zeeman field H parallel (top) and perpendicular (bottom) to the principal symmetry axes. The red numbers are as described above. Red arrows mark the observed EPR transition assignment.

dx.doi.org/10.1021/ja5043116 | J. Am. Chem. Soc. 2014, 136, 11964−11971

by $g_\perp = g_\perp'/2$ and $g_\parallel = g_\parallel'$,[27] thus the actual g values are g_x = 3.32, g_y = 3.18, and g_z = 2.91. These are similar to the g values reported for other Fe complexes.[11a,25,26,28]

It can be seen that there is a good agreement between the computer simulated and experimental spectra. The parameters used to fit the experimental spectra were: $S = 3/2$, g_x = 3.34, g_y = 3.32, g_z = 2.91, and D = 20.4 cm^{-1}. Similar magnetic parameters are used to fit the 240 GHz spectrum as shown in Figure S8. Additionally, these data are in agreement with the susceptibility results. Importantly, they provide unambiguous proof that D is positive in this case since a negative D would not generate detectable EPR signals as explained above. As a corollary, the results for **2** provide indirect support that the D value for **3** must be large and negative, as mentioned earlier.

It is generally believed that a weak ligand field gives rise to the unquenched orbital angular momentum in transition-metal complexes. A low coordination number, symmetric coordination environment, and low oxidation state of the metal lead to such a scenario.[29] The recently reported $[Fe(C(SiMe_3)_3)_2]^-$ complex[12a] showing slow magnetic relaxation below 29 K in a zero-applied dc field supported this view. But the present example **3**, even though it holds all the above-mentioned features, shows slow magnetic relaxation only below 4 K at an applied field. In order to get further insight into the local electronic and magnetic behavior we performed CASSCF/CASPT2/RASSI-SO *ab initio* calculations on compounds **1**−**3** using the MOLCAS program package.[30] Computational details are given in the SI.

For **1**, the multiconfigurational *ab initio* calculations show that iron has a clear 3d^6 character, i.e., it is Fe(II) as expected (further explanations given in SI). For **2**, *ab initio* calculations clearly reveal a Fe(I) valence state with a 3d^7 electronic configuration ($S = 3/2$) in the ground state, in accordance with the experimental SQIUD and Mössbauer data. Addition of the ligand bonding/antibonding orbitals of the bonded carbon atoms and/or chlorine atom into the active space of the CASSCF method does not change this picture, although simultaneous addition of all these orbitals into the active space (which would be preferable) is computationally not possible. The spin density population analysis shows that there are three unpaired electrons on the Fe site. It seems that although the Fe−C bond in **2** is significantly shorter than in **1**, it is not sufficient to induce charge-transfer processes which would affect the oxidation state of the metal site. Accordingly, the ground term is ^{4}F, subject to ligand-field splitting. The splitting pattern of this manifold in a nearly trigonal field affords ^{4}A + ^{4}E as the most important three low-lying orbital states. Given the fact that Fe(I) has a slightly weaker spin−orbit coupling constant than Fe(II),[20d] and smaller than the energy separation between the ground ^{4}A and the two excited orbital states (^{4}E, ∼1300 cm^{-1}), the spin−orbit coupling is, in this case, of intermediate strength. The calculated zero-field splitting of the ground state ^{4}A is strongly dependent on the computational model employed and on the electron correlation considered.

For **3**, ab initio calculations reveal an almost net d^7 character of the ground state, again consistent with the experimental SQUID and Mössbauer data. As in **2**, the peculiarity of the ligand field created by the carbene is a relatively small energy splitting of the ground atomic multiplet ^{4}F. The main difference between **2** and **3** is that the ligand field is even smaller (weaker) in the latter. This is partially due to the presence of an additional ligating atom (Cl) which acts as a perturbant with combined effect on the central Fe, electrostatic (formal charge −1) and covalent. Another splitting effect comes from the departure of the C−Fe−C angle from 180°. Due to this relatively small splitting of the entire ^{4}F manifold (≈5000 cm^{-1}), the spin−orbit interaction in **3** is very important, and its effect is strongly dependent on the calculated orbital splitting of the ground atomic multiplet. Accurate (quantitative) account of this effect requires the including of more orbitals into the active space of the CASSCF method than we can currently afford. Further work in this direction is in progress. Qualitatively, however, we can understand the reason why cationic **3** is a much worse molecular magnet compared to Long's $[Fe(C(SiMe_3)_3)_2]^-$ anion.[12a] The reason for this lies in the fundamentally different electronic structure of **3** compared to $[Fe(C(SiMe_3)_3)_2]^-$, which mainly arises from the very different electronic structure of the bonding carbon atoms. In $[Fe(C(SiMe_3)_3)_2]^-$ the bonding carbon atoms have sp^3 hybridization and the main interaction with the Fe atom occurs via a single σ bond, which is collinear to the symmetry axis of the complex. This affords an almost degenerate ^{4}E orbital doublet in the ground state, which leads further, via first order spin−orbit coupling, to very axial ground and first excited Kramers doublets ($g_{x,y} < 10^{-4}$), explaining the high-blocking barrier in this compound. In **3** the situation is quite different: the bonding carbon atoms have sp^2 hybridization, while the interaction with the central Fe atom involves at least the σ and one π_z orbitals of the bonded carbon atoms. Since the π_z orbital is perpendicular to the main σ bond, its effect on the axiality of the Fe(I) will be strongly destructive, as it induces large values of the $g_{x,y}$ component of the ground Kramers doublet state.

In conclusion, we have prepared three- and two-coordinate Fe complexes, $(cAAC)_2FeCl$ (**2**) and $[(cAAC)_2Fe][B(C_6F_5)_4]$ (**3**), respectively. **2** shows a trigonal planar geometry, while **3** is linear. A combination of SQUID, Mössbauer, HF-EPR, and theoretical studies reveals that **2** and **3** have iron atoms in the +1 oxidation state with a spin ground state of $S = 3/2$. **2** represents a rare example of a three-coordinate Fe(I) complex with a nonchelating ligand environment. The chemical structure of **3** shows the first example of a cationic two-coordinate Fe(I) complex. Magnetic studies reveal the slow magnetic relaxation of **2** and **3** under an applied dc magnetic filed typical for SMM behavior. High-frequency EPR measurements reveal easy plane anisotropy for compound **2**. Theoretical studies suggest that carbon atoms bonded to Fe(I) in **3** have sp^2 hybridization and so the π_z orbital on the carbene carbon atom destructively affects the magnetic axiality of Fe(I). Interestingly, the attenuated SMM character of **3** compared to Long's $[Fe(C(SiMe_3)_3)_2]^-$ shows that there can be no general and simple rule to predict the design of a SMM solely based on coordination number, symmetry of the coordination environment, and low oxidation state of the metal.

■ EXPERIMENTAL SECTION

Syntheses were carried out under an inert gas atmosphere of dinitrogen in oven-dried glassware using standard Schlenk techniques. Other manipulations were accomplished in a dinitrogen-filled glovebox. Solvents were purified by MBRAUN solvent purification system MB SPS-800. Fluorobenzene was dried by refluxing with calcium dihydride. All chemicals were purchased from Aldrich and used without further purification. cAAC was prepared following the reported procedure.[31] Elemental analyses were carried out in the Analytisches Labor der Anorganischen Chemie der Universität Göttingen. Experimental details of crystal structure determination, SQIUD magnetic measurements, and Mössbauer spectroscopy and

dx.doi.org/10.1021/ja5043116 | J. Am. Chem. Soc. 2014, 136, 11964−11971

methods used for theoretical calculations are provided in the Supporting Information.

Synthesis of 1. To a mixture of $FeCl_2$ (0.252 g, 2 mmol) and cAAC (1.14 g, 4 mmol), THF (8 mL) was added at room temperature, and the mixture was stirred for 16 h. The turbid yellow-orange solution was filtered through a frit and **1** was collected as precipitate. Storing a saturated solution of **1** in toluene at 0 °C afforded crystals suitable for X-ray diffraction. (Yield: 62%, 0.864 g). Mp 135 °C (decomp.). Elemental analysis (%) calcd for $C_{40}H_{62}Cl_2FeN_2$ (696.36): C, 68.86; H, 8.96; N, 4.02. Found: C, 67.80; H, 8.80; N, 3.99.

Synthesis of 2. Precooled THF (30 mL, −78 °C) was added to a mixture of **1** (0.697 g, 1 mmol) and KC_8 (0.135 g, 1 mmol), and the solution was stirred for 1.5 h while allowing the temperature to rise slowly. After reaching room temperature, stirring was continued for another 15 min, and the solution was filtered to remove the graphite. The red solution was subjected to reduced pressure to remove THF, and the dark red residue was extracted with toluene (100 mL). The solution was concentrated and stored at −18 °C to afford single crystals of **2** suitable for X-ray diffraction. (Yield: 71%, 0.47 g). Mp 181 °C (decomp.). Elemental analysis (%) calcd for $C_{40}H_{62}ClFeN_2$ (661.40): C, 72.55; H, 9.44; N, 4.23. Found: C, 71.72; H, 9.67; N, 4.15.

Synthesis of 3. To a mixture of **2** (0.200 g, 0.3 mmol) and $Li[B(C_6F_5)_4]\cdot 2.5\ Et_2O$ (0.271 g, 0.3 mmol), precooled toluene (50 mL, −78 °C) was added while stirring. The temperature of the solution was allowed to rise slowly within 1 h. The final temperature was kept below 15 °C. The precipitated blue compound **3** was collected by filtration, and single crystals suitable for X-ray diffraction were obtained from a saturated solution in fluorobenzene at −32 °C. (Yield: 90%, 0.35 g). Mp 145 °C (decomp.). Elemental analysis (%) calcd for $C_{64}H_{62}BF_{20}FeN_2$ (1305.40): C, 58.87; H, 4.79; N, 2.15. Found: C, 58.99; H, 4.89; N, 2.11.

■ ASSOCIATED CONTENT

Ⓢ Supporting Information

The cif files of **1**−**3**, and the details of crystal structure refinements, magnetic measurements, Mössbauer spectroscopy, EPR and theoretical investigations. This material is available free of charge via the Internet at http://pubs.acs.org.

■ AUTHOR INFORMATION

Corresponding Authors

hroesky@gwdg.de
dstalke@chemie.uni-goettingen.de
franc.meyer@chemie.uni-goettingen.de
liviu.ungur@chem.kuleuven.be
dalal@chem.fsu.edu

Notes

The authors declare no competing financial interest.

■ ACKNOWLEDGMENTS

H.W.R. thanks the Deutsche Forschungsgemeinschaft for financial support (RO 224/60-1). D.S. thanks the DNRF-funded Center for Materials Crystallography (CMC) for partial funding. L.U. is a postdoc of the Flemish Science Foundation (FWO-Vlaanderen) and also acknowledges the support from the INPAC and Methusalem programs of the KU Leuven. HF-EPR measurements were carried out at the NHMFL, which is supported by a NSF National Science Foundation Cooperative agreement no. DMR-0654118, the State of Florida, and the U.S. Department of Energy. We thank Dr. A. C. Stückl for X-band EPR measurements. This paper is dedicated to Professor Tobin J. Marks on the occasion of his 70th birthday.

■ REFERENCES

(1) Lindley, P. F. *Rep. Prog. Phys.* **1996**, *59*, 867−933.

(2) (a) Holland, P. L. *Acc. Chem. Res.* **2008**, *41*, 905−914. (b) Power, P. P. *Chem. Rev.* **2012**, *112*, 3482−3507.

(3) (a) Högbom, M.; Huque, Y.; Sjöberg, B.-M.; Nordlund, P. *Biochemistry* **2002**, *41*, 1381−1389. (b) Peters, J. W.; Fischer, K.; Dean, D. R. *Annu. Rev. Microbiol.* **1995**, *49*, 335−366.

(4) Bradley, D. C.; Chisholm, M. H. *Acc. Chem. Res.* **1976**, *9*, 273−280.

(5) Bradley, D. C.; Hursthouse, M. B.; Rodesiler, P. F. *Chem. Commun.* **1969**, 14−15.

(6) (a) Power, P. P.; Shoner, S. C. *Angew. Chem.* **1991**, *103*, 308−309. (b) Bartlett, R. A.; Ellison, J. J.; Power, P. P.; Shoner, S. C. *Inorg. Chem.* **1991**, *30*, 2888−2894. (c) Olmstead, M. M.; Power, P. P.; Shoner, S. C. *Inorg. Chem.* **1991**, *30*, 2547−2551. (d) MacDonnell, F. M.; Ruhlandt-Senge, K.; Ellison, J. J.; Holm, R. H.; Power, P. P. *Inorg. Chem.* **1995**, *34*, 1815−1822.

(7) (a) Roddick, D. M.; Tilley, T. D.; Rheingold, A. L.; Geib, S. J. *J. Am. Chem. Soc.* **1987**, *109*, 945−946. (b) Stokes, S. L.; Davis, W. M.; Odom, A. L.; Cummins, C. C. *Organometallics* **1996**, *15*, 4521−4530. (c) O'Donoghue, M. B.; Zanetti, N. C.; Davis, W. M.; Schrock, R. R. *J. Am. Chem. Soc.* **1997**, *119*, 2753−2754. (d) Putzer, M. A.; Neumueller, B.; Behnicke, K.; Magull, J. *Chem. Ber.* **1996**, *129*, 715−719. (e) Siemeling, U.; Vorfeld, U.; Neumann, B.; Stammler, H.-G. *Inorg. Chem.* **2000**, *39*, 5159−5160.

(8) (a) Andres, H.; Bominaar, E. L.; Smith, J. M.; Eckert, N. A.; Holland, P. L.; Münck, E. *J. Am. Chem. Soc.* **2002**, *124*, 3012−3025. (b) Holland, P. L.; Cundari, T. R.; Perez, L. L.; Eckert, N. A.; Lachicotte, R. J. *J. Am. Chem. Soc.* **2002**, *124*, 14416−14424. (c) Eckert, N. A.; Smith, J. M.; Lachicotte, R. J.; Holland, P. L. *Inorg. Chem.* **2004**, *43*, 3306−3321. (d) Gregory, E. A.; Lachicotte, R. J.; Holland, P. L. *Organometallics* **2005**, *24*, 1803−1805.

(9) (a) Brown, S. D.; Betley, T. A.; Peters, J. C. *J. Am. Chem. Soc.* **2003**, *125*, 322−323. (b) Kisko, J. L.; Hascall, T.; Parkin, G. *J. Am. Chem. Soc.* **1998**, *120*, 10561−10562.

(10) Stoian, S. A.; Yu, Y.; Smith, J. M.; Holland, P. L.; Bominaar, E. L.; Münck, E. *Inorg. Chem.* **2005**, *44*, 4915−4922.

(11) (a) Chiang, K. P.; Scarborough, C. C.; Horitani, M.; Lees, N. S.; Ding, K.; Dugan, T. R.; Brennessel, W. W.; Bill, E.; Hoffman, B. M.; Holland, P. L. *Angew. Chem., Int. Ed.* **2012**, *51*, 3658−3662. (b) Rodriguez, M. M.; Stubbert, B. D.; Scarborough, C. C.; Brennessel, W. W.; Bill, E.; Holland, P. L. *Angew. Chem., Int. Ed.* **2012**, *51*, 8247−8250.

(12) (a) Zadrozny, J. M.; Xiao, D. J.; Atanasov, M.; Long, G. J.; Grandjean, F.; Neese, F.; Long, J. R. *Nat. Chem.* **2013**, *5*, 577−581. (b) Murrie, M. *Chem. Soc. Rev.* **2010**, *39*, 1986−1995.

(13) (a) Pelties, S.; Wolf, R. *Z. Anorg. Allg. Chem.* **2013**, *639*, 2581−2585. (b) Samuel, P. P.; Mondal, K. C.; Roesky, H. W.; Hermann, M.; Frenking, G.; Demeshko, S.; Meyer, F.; Stückl, A. C.; Christian, J. H.; Dalal, N. S.; Ungur, L.; Chibotaru, L. F.; Pröpper, K.; Meents, A.; Dittrich, B. *Angew. Chem., Int. Ed.* **2013**, *52*, 11817−11821.

(14) Kottke, T.; Stalke, D. *J. Appl. Crystallogr.* **1993**, *26*, 615−619.

(15) Bart, S. C.; Chłopek, K.; Bill, E.; Bouwkamp, M. W.; Lobkovsky, E.; Neese, F.; Wieghardt, K.; Chirik, P. J. *J. Am. Chem. Soc.* **2006**, *128*, 13901−13912.

(16) Gütlich, P.; Bill, E.; Trautwein, A. X. *Mössbauer Spectroscopy and Transition Metal Chemistry - Fundamentals and Applications*; Springer: Heidelberg, 2011.

(17) (a) Eichhöfer, A.; Lan, Y.; Mereacre, V.; Bodenstein, T.; Weigend, F. *Inorg. Chem.* **2014**, *53*, 1962−1974. (b) Sanakis, Y.; Power, P. P.; Stubna, A.; Münck, E. *Inorg. Chem.* **2002**, *41*, 2690−2696. (c) Evans, D. J.; Hughes, D. L.; Silver, J. *Inorg. Chem.* **1997**, *36*, 747−748.

(18) Gomez-Coca, S.; Cremades, E.; Aliaga-Alcalde, N.; Ruiz, E. *J. Am. Chem. Soc.* **2013**, *135*, 7010−7018.

(19) Zadrozny, J. M.; Liu, J.; Piro, N. A.; Chang, C. J.; Hill, S.; Long, J. R. *Chem. Commun.* **2012**, *48*, 3927−3929.

(20) (a) Huang, W.; Liu, T.; Wu, D.; Cheng, J.; Ouyang, Z. W.; Duan, C. *Dalton Trans.* **2013**, *42*, 15326−15331. (b) Vallejo, J.;

Castro, I.; Ruiz-García, R.; Cano, J.; Julve, M.; Lloret, F.; De Munno, G.; Wernsdorfer, W.; Pardo, E. *J. Am. Chem. Soc.* **2012**, *134*, 15704−15707. (c) Colacio, E.; Ruiz, J.; Ruiz, E.; Cremades, E.; Krzystek, J.; Carretta, S.; Cano, J.; Guidi, T.; Wernsdorfer, W.; Brechin, E. K. *Angew. Chem., Int. Ed.* **2013**, *52*, 9130−9134. (d) Abragam, A.; Bleaney, B. *Electronic Paramagnetic Resonance of Transition Ions*; Clarendon: Oxford, 1970.

(21) (a) Reiff, W. M.; LaPointe, A. M.; Witten, E. H. *J. Am. Chem. Soc.* **2004**, *126*, 10206−10207. (b) Merrill, W. A.; Stich, T. A.; Brynda, M.; Yeagle, G. J.; Fettinger, J. C.; De Hont, R.; Reiff, W. M.; Schulz, C. E.; Britt, R. D.; Power, P. P. *J. Am. Chem. Soc.* **2009**, *131*, 12693−12702.

(22) Lin, C.-Y.; Guo, J.-D.; Fettinger, J. C.; Nagase, S.; Grandjean, F.; Long, G. J.; Chilton, N. F.; Power, P. P. *Inorg. Chem.* **2013**, *52*, 13584−13593.

(23) Hill, S.; Perenboom, J. A. A. J.; Dalal, N. S.; Hathaway, T.; Stalcup, T.; Brooks, J. S. *Phys. Rev. Lett.* **1998**, *80*, 2453−2456.

(24) Perenboom, J. A. A. J.; Brooks, J. S.; Hill, S.; Hathaway, T.; Dalal, N. S. *Phys. Rev. B* **1998**, *58*, 330−338.

(25) Cowley, R. E.; Bill, E.; Neese, F.; Brennessel, W. W.; Holland, P. L. *Inorg. Chem.* **2009**, *48*, 4828−4836.

(26) (a) Krzystek, J.; Ozarowski, A.; Telser, J. *Coord. Chem. Rev.* **2006**, *250*, 2308−2324. (b) Krzystek, J.; Zvyagin, S. A.; Ozarowski, A.; Trofimenko, S.; Telser, J. *J. Magn. Reson.* **2006**, *178*, 174−183.

(27) (a) Weltner, W., Jr. *Magnetic Atoms and Molecules*; Van Nostrand-Reinhold: New York, 1983. (b) Chen, W.-Z.; Cotton, F. A.; Dalal, N. S.; Murillo, C. A.; Ramsey, C. M.; Ren, T.; Wang, X. *J. Am. Chem. Soc.* **2005**, *127*, 12691−12696.

(28) (a) Solano-Peralta, A.; Saucedo-Vazquez, J. P.; Escudero, R.; Höpfl, H.; El-Mkami, H.; Smith, G. M.; Sosa-Torres, M. E. *Dalton Trans.* **2009**, 1668−1674. (b) Yatsunyk, L. A.; Walker, F. A. *Inorg. Chem.* **2004**, *43*, 757−777. (c) Branca, M.; Culeddu, N.; Fruianu, M.; Marchettini, N.; Tiezzi, E. *Magn. Reson. Chem.* **1997**, *35*, 687−690. (d) de Abreu, C. D.; Pinhal, N. M.; Vugman, N. V. *J. Magn. Reson.* **1992**, *100*, 588−592.

(29) (a) Dey, M.; Gogoi, N. *Angew. Chem., Int. Ed.* **2013**, *52*, 12780−12782. (b) Bill, E. *Nat. Chem.* **2013**, *5*, 556−557.

(30) (a) Aquilante, F.; De Vico, L.; Ferre, N.; Ghigo, G.; Malmqvist, P. -Å.; Neogrady, P.; Pedersen, T. B.; Pitonak, M.; Reiher, M.; Roos, B. O.; Serrano-Andres, L.; Urban, M.; Veryazov, V.; Lindh, R. *J. Comput. Chem.* **2010**, *31*, 224−247 www.molcas.org. (b) Malmqvist, P. -Å.; Roos, B. O.; Schimmelpfennig, B. *Chem. Phys. Lett.* **2002**, *357*, 230−240.

(31) (a) Lavallo, V.; Canac, Y.; Präsang, C.; Donnadieu, B.; Bertrand, G. *Angew. Chem., Int. Ed.* **2005**, *44*, 5705−5709. (b) Jazzar, R.; Dewhurst, R. D.; Bourg, J.-B.; Donnadieu, B.; Canac, Y.; Bertrand, G. *Angew.Chem. Int. Ed.* **2007**, *46*, 2899−2902.

■ NOTE ADDED IN PROOF

While reading the proof of this article, we realized that another manuscript describing cAAC stabilized Fe(I) complexes had been submitted in the meantime (DOI: 10.1002/ange.201404078).